EXTENDED PDF FORMAT
SPONSORED BY

BIO-RAD

http://discover.bio-rad.com

Facile Splitting of Hydrogen and Ammonia by Nucleophilic Activation at a Single Carbon Center

Guido D. Frey, *et al.*

Science **316**, 439 (2007);
DOI: 10.1126/science.1141474

The following resources related to this article are available online at www.sciencemag.org (this information is current as of April 20, 2007):

Updated information and services, including high-resolution figures, can be found in the online version of this article at:
http://www.sciencemag.org/cgi/content/full/316/5823/439

Supporting Online Material can be found at:
http://www.sciencemag.org/cgi/content/full/316/5823/439/DC1

This article **cites 32 articles**, 3 of which can be accessed for free:
http://www.sciencemag.org/cgi/content/full/316/5823/439#otherarticles

This article appears in the following **subject collections**:
Chemistry
http://www.sciencemag.org/cgi/collection/chemistry

Information about obtaining **reprints** of this article or about obtaining **permission to reproduce this article** in whole or in part can be found at:
http://www.sciencemag.org/about/permissions.dtl

Downloaded from www.sciencemag.org on April 20, 2007

Science (print ISSN 0036-8075; online ISSN 1095-9203) is published weekly, except the last week in December, by the American Association for the Advancement of Science, 1200 New York Avenue NW, Washington, DC 20005. Copyright c 2007 by the American Association for the Advancement of Science; all rights reserved. The title SCIENCE is a registered trademark of AAAS.

high-pressure experiments, we anticipated observing this effect in our hardness measurements as well. Indeed, Fig. 2A shows that there is a substantial difference between the highest and lowest measured hardness across grains of ReB_2 under the same load. This observed spread in hardness values at constant load can be attributed to the anisotropic structure of ReB_2, combined with our inability to control the crystallographic orientation of the tested grains. For example, under a load of 4.9 N, the highest measured hardness is 32.5 GPa and the lowest obtained value is 26.0 GPa.

We can begin to understand this variation in hardness by using electron backscattering diffraction to measure the orientations of the grains studied (Fig. 2, C and D). The results indicate that indentations parallel to the (00*l*) planes yielded the lowest average hardness, a value of 27 GPa. In contrast, indentations along directions that contained a larger component parallel to the *c* axis [that is, perpendicular to (00*l*)] resulted in measurements with an average hardness of 31 GPa, an increase of 15%. The dependence of hardness data on crystallographic orientation can be explained by the presence of the same slip planes described above. Furthermore, because similar anisotropic behavior is observed in the high-pressure data, we conclude that the radial diffraction study elucidates the plastic behavior of the material, giving an indication of the yield strength rather than merely measuring elastic behavior.

In our microindentation experiments to date, we have found no grains with pure (00*l*) orientation. As a result, our data demonstrate a minimum average hardness. It is likely that these planes parallel to (00*l*), which we were unable to directly measure, will have an even higher hardness and are responsible for scratching diamond (Fig. 2B).

References and Notes

1. P. F. McMillan, *Nat. Mater.* **1**, 19 (2002).
2. D. He *et al.*, *Appl. Phys. Lett.* **81**, 643 (2002).
3. V. L. Solozhenko, D. Andrault, G. Fiquet, M. Mezouar, D. C. Rubie, *Appl. Phys. Lett.* **78**, 1385 (2001).
4. R. W. Cumberland *et al.*, *J. Am. Chem. Soc.* **127**, 7264 (2005).
5. Incompressibility is the resistance to elastic volume compression and is reported as bulk modulus in units of gigapascals. Hardness is resistance to plastic deformation and is reported in units of force per unit area (in gigapascals).
6. R. B. Kaner, J. J. Gilman, S. H. Tolbert, *Science* **308**, 1268 (2005).
7. H. Cynn, J. E. Klepeis, C.-S. Yoo, D. A. Young, *Phys. Rev. Lett.* **88**, 135701 (2002).
8. F. Occelli *et al.*, *Phys. Rev. Lett.* **93**, 95502 (2004).
9. T. Kenichi, *Phys. Rev. B* **70**, 12101 (2004).
10. I. V. Aleksandrov, E. F. Goncharov, A. N. Zisman, S. M. Stishov, *Sov. Phys. JETP* **66**, 384 (1987).
11. H. J. McSkimin, W. L. Bond, *Phys. Rev.* **105**, 116 (1957).
12. M. H. Manghnani, K. Katahara, E. S. Fisher, *Phys. Rev. B* **9**, 1421 (1974).
13. C. A. Hampel, *Rare Metals Handbook* (Reinhold, London, 1961).
14. C. G. Fink, P. Deren, *Trans. Electro-chem. Soc.* **66**, 381 (1934).
15. A. Vegas, L. A. Martinez-Cruz, A. Ramos-Gallardo, A. Romero, *Z. Kristallogr.* **210**, 574 (1995).
16. S. La Placa, B. Post, *Acta Crystallogr.* **15**, 97 (1962).
17. Y. Z. Chen, H. J. Xiang, J. Yang, J. G. Hou, Q. Zhu, *Phys. Rev. B* **74**, 12102 (2006).
18. M. Hebbache, L. Stuparevic, D. Zivkovic, *Solid State Commun.* **139**, 227 (2006).
19. S. Chiodo, H. J. Gotsis, N. Russo, E. Sicilia, *Chem. Phys. Lett.* **425**, 311 (2006).
20. H. Gou *et al.*, *Appl. Phys. Lett.* **88**, 221904 (2006).
21. L. Rao, E. G. Gillan, R. B. Kaner, *J. Mater. Res.* **10**, 353 (1995).
22. H. Gao, Y. Huang, W. D. Nix, *Naturwissenschaften* **86**, 507 (1999).
23. A. L. Ruoff, *J. Appl. Phys.* **46**, 1389 (1975).
24. A. K. Singh, *J. Appl. Phys.* **73**, 4278 (1993).
25. A. K. Singh, C. Balasingh, H. K. Mao, R. J. Hemley, J. F. Shu, *J. Appl. Phys.* **83**, 7567 (1998).
26. B. Kiefer, S. R. Shieh, T. S. Duffy, T. Sekine, *Phys. Rev. B* **72**, 14102 (2005).
27. D. He, S. R. Shieh, T. S. Duffy, *Phys. Rev. B* **70**, 184121 (2004).
28. G. M. Amulele, M. H. Manghnani, M. J. Somayazulu, *J. Appl. Phys.* **99**, 23522 (2006).
29. This work was funded by NSF under grants DMR-0453121 (R.B.K.), EAR-0510914 (A.K.), and CMS-0307322 (S.H.T.), and an Integrative Graduate Education and Research Traineeship (J.B.L.). Use of the National Synchrotron Light Source, Brookhaven National Laboratory, and the Advanced Light Source, Lawrence Berkeley National Laboratory, were supported by the U.S. Department of Energy, Office of Basic Energy Science, under contracts DE-AC02-98CH10886 and DE-AC03-76SF00098, respectively. The authors thank S. Caldwell, S. Clark, R. Cumberland, S. Fakra, J. Gilman, J. Hu, M. Kunz, and A. Phan for their assistance with this research.

Supporting Online Material
www.sciencemag.org/cgi/content/full/316/5823/436/DC1
Materials and Methods
Fig. S1

26 December 2006; accepted 16 March 2007
10.1126/science.1139322

Facile Splitting of Hydrogen and Ammonia by Nucleophilic Activation at a Single Carbon Center

Guido D. Frey, Vincent Lavallo, Bruno Donnadieu, Wolfgang W. Schoeller,* Guy Bertrand*

In possessing a lone pair of electrons and an accessible vacant orbital, singlet carbenes resemble transition metal centers and thus could potentially mimic their chemical behavior. Although singlet di(amino)carbenes are inert toward dihydrogen, it is shown that more nucleophilic and electrophilic (alkyl)(amino)carbenes can activate H_2 under mild conditions, a reaction that has long been known for transition metals. However, in contrast to transition metals that act as electrophiles toward dihydrogen, these carbenes primarily behave as nucleophiles, creating a hydride-like hydrogen, which then attacks the positively polarized carbon center. This nucleophilic behavior allows these carbenes to activate NH_3 as well, a difficult task for transition metals because of the formation of Lewis acid-base adducts.

The activation of enthalpically strong small molecules such as molecular hydrogen (H_2) and ammonia (NH_3) has attracted considerable interest over the years. The first observation of H_2 splitting dates from the end of the 19th century, when Sabatier observed the formation of ethane in the addition of H_2 to ethylene over thin slivers of lightly heated reduced nickel (*1*). Since that time, most of the chemical and biological systems that have been found to split H_2 involve a transition metal center. Even for the so-called iron-sulfur cluster-free hydrogenase (Hmd), it has recently been shown that an iron center was of functional importance (*2*, *3*). The only nonmetallic systems reported to cleave H_2 under mild experimental conditions (*4*–*7*) are phosphine-borane species (*8*, *9*) and a stable digermyne (*10*).

In contrast to dihydrogen, ammonia usually forms simple Lewis acid-base adducts with transition metal complexes, as observed first by Werner in the late 19th century, because of the presence of a lone pair of electrons at nitrogen (*11*). Consequently, examples of NH_3 splitting are still very rare (*12*–*17*).

The activation of H-X and particularly H-H bonds requires that the pair of bonding electrons be perturbed in some way so as to form a chemically active species. The digermyne has substantial diradical character and therefore reacts through H atom abstraction from H_2, followed by recombination of the resultant radical pair (*10*). In contrast, the splitting of H_2 at a transition metal center results from the primary interaction of a vacant orbital at the metal and the σ-bonding orbital of H_2 (*18*–*22*) (Fig. 1). When concomitant back-donation from a filled *d* orbital to the anti-bonding σ* orbital of the bound H_2 is sufficiently strong, homolytic bond cleavage occurs. Otherwise, the acidic η^2-H_2 ligand undergoes proton transfer to another

---

UCR-CNRS Joint Research Chemistry Laboratory (UMI 2957), Department of Chemistry, University of California, Riverside, CA 92521–0403, USA.

*To whom correspondence should be addressed. E-mail: gbertran@mail.ucr.edu

metal-bound ligand. This latter type of process is often referred to as heterolytic cleavage and is also probably operative for phosphine-borane–containing species (*8*, *9*, *23*).

A singlet carbene has a vacant orbital and a filled nonbonding orbital (*24*, *25*) and in that respect resembles transition metal centers. Although the spatial disposition of a carbene's orbitals is not as ideally suited for interaction with hydrogen as that of a metal, we reasoned that sufficient overlap might still occur and thus enable activation of H_2 (Fig. 1).

Herein we report that stable, singlet, acyclic and cyclic (alkyl)(amino)carbenes **1** (*26*) and **2** (*27*) undergo a formal oxidative addition of H_2. Calculations predict that the transition state results from the primary interaction of the carbene's lone pair of electrons with an H_2 antibonding orbital; thus, the carbene acts as a base toward H_2, creating a hydridelike hydrogen that attacks the positively polarized carbon center. This hypothesis of a nucleophilic activation process is reinforced by observation of the reaction of **1** and **2** with NH_3. Because of the strong nucleophilic character of these carbenes, no "Werner-like" adducts can be formed, and hence N-H bond cleavage occurs smoothly.

It has already been shown that cyclic di(amino)carbenes (NHCs) (*28*, *29*) do not react with H_2 (*30*) nor with CO (*31*), whereas the latter adds to both acyclic and cyclic (alkyl)(amino)carbenes **1** and **2** (*32*). According to our calculations (*33*), the highest occupied molecular orbital (HOMO) and the singlet-triplet gap for the model mono(amino)carbenes (**1′**, **2′**, and **2″**) are slightly higher and significantly smaller in energy, respectively, than those of NHC **3′** and acyclic di(amino)carbene **4′** (Table 1). Consequently, carbenes **1** and **2** are slightly more nucleophilic, but considerably more electrophilic (*34*), than NHCs **3** and are therefore better candidates for transition metal–like behavior. This hypothesis was borne out upon bubbling H_2 through a solution of (alkyl)(amino)carbenes **1** and **2** at 35°C, because clean reactions occurred, and after purification adducts **5** and **6** were obtained in ~30% yield (*35*) as colorless crystals (Fig. 2A). All compounds were fully characterized by standard spectroscopic methods, including a single crystal x-ray diffraction study for **6a** (fig. S1) (*36*). We confirmed that cyclic bis(amino)carbene **3** (*37*) does not react with hydrogen under our experimental conditions and found that the acyclic version **4** (*38*) is similarly inert.

The calculated energy changes (ΔE) (Fig. 4, Table 1, and table S3) show that although the reactions of all carbenes with H_2 are exothermic, the reactions are significantly more favored for mono(amino)carbenes (**1′**, **2′**, and **2″**) than for di(amino)carbenes (**3′** and **4′**). More importantly, the activation energy is at least 40 kJ/mol lower in the case of the mono(amino)carbenes, which readily rationalizes our experimental results.

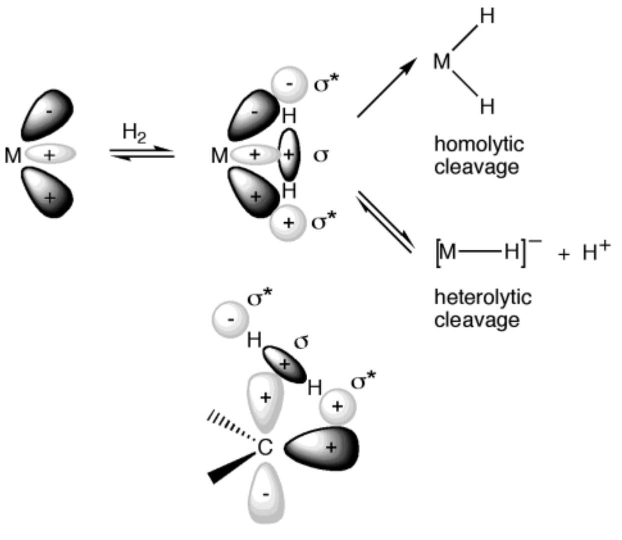

Fig. 1. Schematic representations of modes of activation of H_2 at a transition metal center (**top**) and a hypothetical extrapolation of a similar process at a carbene carbon (**bottom**); filled orbitals are in black, and vacant orbitals in gray.

Table 1. Calculated energy of the HOMO (E_{HOMO}) and singlet-triplet energy gap [$-(E_S - E_T)$] for the model carbenes shown in Fig. 4, as well as energy changes (ΔE) and activation energies ($\Delta E^‡$) for their reactions with H_2 and NH_3 calculated at the B3LYP/6-311 g** level of theory.

	1′	2′	2″	3′	4′
E_{HOMO} (eV)	–5.0	–5.0	–4.9	–5.2	–5.1
$-(E_S - E_T)$ (kj/mol)	139.2	193.5	188.9	285.1	214.0
$\Delta E(H_2)$ (kj/mol)	–211.8	–189.4	–180.0	–106.3	–121.0
$\Delta E(H_2)^‡$ (kj/mol)	93.0	99.1	108.3	150.0	147.8
$\Delta E(NH_3)$ (kj/mol)	–161.9	–139.3		–70.8	–73.4
$\Delta E(NH_3)^‡$ (kj/mol)	87.4	94.5		141.3	137.5

For the addition of H_2 to model compound **2′**, we further calculated the geometric parameters of potential intermediate structures along the reaction pathway (Fig. 2B). According to the lowest energy simulated trajectory, the H_2 molecule approaches the carbene as depicted in Fig. 2B. In the transition state, the H-H bond distance (1.071 Å) is comparable to those found for purely σ-bonded H_2 transition metal complexes (1.0 to 1.2 Å) (compare with the bond distance in H_2 gas of 0.77 Å) (*20*). The H_2 molecule becomes polarized, and the positively charged H (+0.178) is already bonded to the carbon (1.206 Å), whereas the pseudohydridic H (–0.195) remains further away at a distance of 1.924 Å. The H-H bond then elongates further (1.388 Å), engendering greater hydridic character (–0.243) to one of the H atoms, which nonetheless remains distant from the carbon center (1.807 Å). Stereochemical inversion at the carbon center then allows the formation of the second C-H bond. This net process is a hybrid between a homolytic and heterolytic cleavage. However, in contrast to the electrophilic activation and proton transfer pathway favored by transition metal centers, carbenes act by initial nucleophilic activation, followed by hydride transfer.

Because H-H and N-H bond dissociation energies are comparable, the main obstacle for the activation of NH_3 by transition metals is the electrophilicity of the metal, which instead favors the formation of Werner-type amine complexes. Having observed the nucleophilic mode of activation of H_2 by mono(amino) carbenes **1** and **2**, we considered it likely that these carbenes would also activate the N-H bond of ammonia, although it is known that NHCs do not (*39*). Our calculations (Table 1 and table S4) predicted comparable reaction barriers to H_2 activation and a less favored, but still exothermic, driving force. Consistent with these computational results, both carbenes **1** and **2** rapidly react with liquid NH_3, even at –40°C, cleanly affording adducts **7** and **8**, respectively (Fig. 3A). The compounds were isolated in >90% yield, and compound **8b** was crystallographically characterized (Fig. 3B).

The mode of approach of NH_3 to **2′** is calculated to be very similar to that observed with H_2. In the transition state, one of the N-H bonds is very long (1.500 Å) and strongly polarized, with the positively charged H (+0.316) tightly bonded to the carbon (1.155 Å) and the pseudo-amide fragment (–1.042) remaining distant from the carbon center (2.314 Å). Importantly, the nitrogen lone pair is pointing away from the carbene vacant orbital, supporting the nucleophilic character of the activation process (Fig. 3B).

The results reported here show that stable singlet carbenes can mimic to some extent the behavior of transition metals. Like the latter, the electronic properties of carbene centers can be

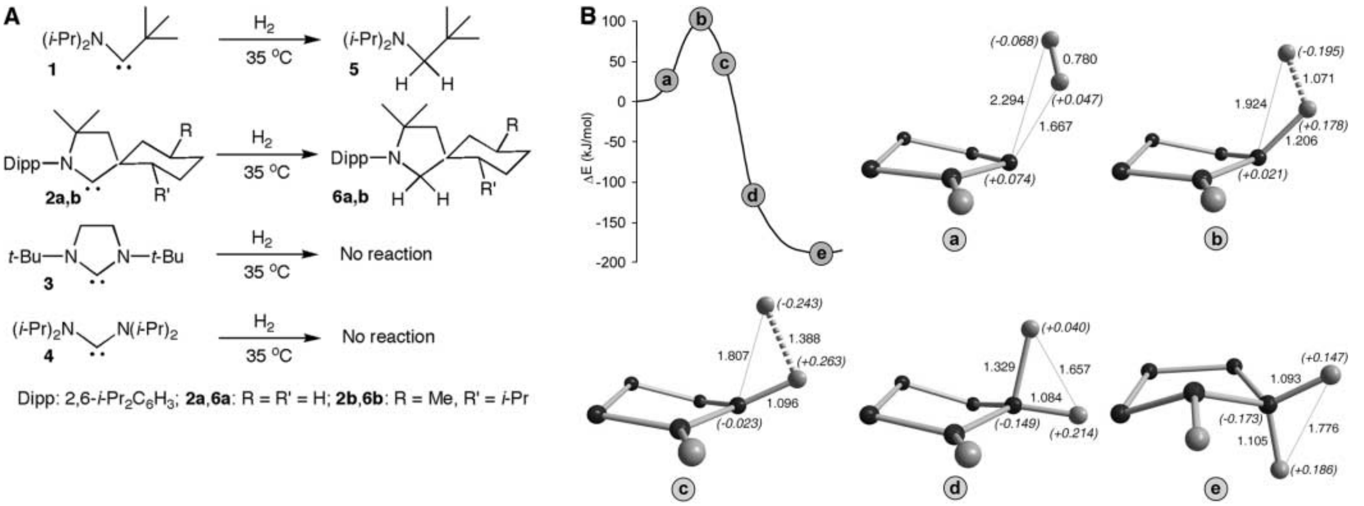

Fig. 2. (**A**) Under mild conditions, (alkyl)(amino)carbenes **1** and **2** activate H_2, whereas (diamino)carbenes **3** and **4** are inert. (**B**) Some structures along the reaction pathway of the insertion of carbene **2′** into H_2, calculated at the B3LYP/6-311 g** level of theory. Bond distances (Å) and charges (in parentheses) are given in the structure drawings, and relative energies are shown in the reaction coordinate diagram.

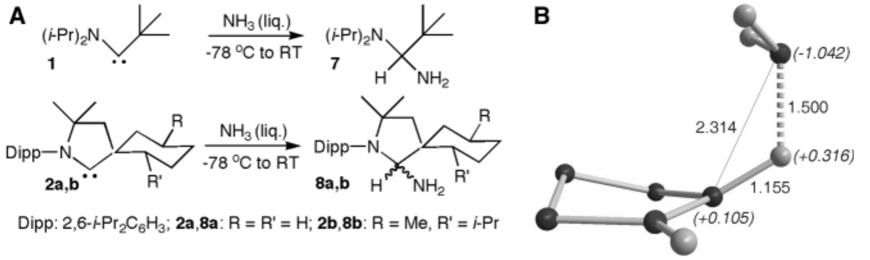

Fig. 3. (**A**) (Alkyl)(amino)carbenes **1** and **2** split ammonia at subzero temperatures. (**B**) Bond distances (Å) and charges (in parentheses) for the transition state of the reaction of NH_3 with carbene **2′**, calculated at the B3LYP/6-311 g** level of theory.

Fig. 4. Model carbenes used for the calculated values shown in Table 1.

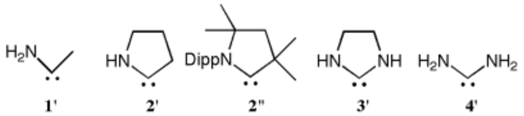

tuned by modifying the nature of the substituents, as shown by the differing reactivities of mono(amino)carbenes and diaminocarbenes with H_2 and NH_3. Moreover, the nucleophilic activation of NH_3, under very mild conditions, offers an alternative paradigm in the continuing search for catalytic systems capable of transforming ammonia efficiently into useful amino compounds.

References and Notes

1. P. Sabatier, *Ind. Eng. Chem.* **18**, 1005 (1926).
2. E. J. Lyon *et al.*, *Eur. J. Biochem.* **271**, 195 (2004).
3. O. Pilak *et al.*, *J. Mol. Biol.* **358**, 798 (2006).
4. A few species, which are only stable in matrices at 10 to 80 K, are also known to split H_2: subvalent group 13 species, (*5*) triplet carbenes (*6*), and the highly electrophilic singlet difluorovinylidene (*7*).
5. H.-J. Himmel, *J. Chem. Soc. Dalton Trans.* **2003**, 3639 (2003).
6. H. Tomioka, in *Reactive Intermediate Chemistry*, R. A. Moss, M. S. Platz, M. Jones Jr., Eds. (Wiley, New York, 2004), pp. 375–461.
7. C. Kötting, W. Sander, *J. Am. Chem. Soc.* **121**, 8891 (1999).
8. G. C. Welch, R. R. San Juan, J. D. Masuda, D. W. Stephan, *Science* **314**, 1124 (2006).
9. G. C. Welch, D. W. Stephan, *J. Am. Chem. Soc.* **129**, 1880 (2007).
10. G. H. Spikes, J. C. Fettinger, P. P. Power, *J. Am. Chem. Soc.* **127**, 12232 (2005).
11. A. Werner, *Z. Anorg. Chem.* **3**, 267 (1893).
12. Y. Nakajima, H. Kameo, H. Suzuki, *Angew. Chem. Int. Ed.* **45**, 950 (2006).
13. J. Zhao, A. S. Goldman, J. F. Hartwig, *Science* **307**, 1080 (2005).
14. E. G. Bryan, B. F. G. Johnson, K. Lewis, *J. Chem. Soc. Dalton Trans.* **1977**, 1328 (1977).
15. G. L. Hillhouse, J. E. Bercaw, *J. Am. Chem. Soc.* **106**, 5472 (1984).
16. A. L. Casalnuovo, J. C. Calabrese, D. Milstein, *Inorg. Chem.* **26**, 941 (1987).
17. M. M. B. Holl, P. T. Wolczanski, G. V. Duyne, *J. Am. Chem. Soc.* **112**, 7989 (1990).
18. G. J. Kubas, R. R. Ryan, B. I. Swanson, P. J. Vergamini, H. J. Wasserman, *J. Am. Chem. Soc.* **106**, 451 (1984).
19. G. J. Kubas, *Adv. Inorg. Chem.* **56**, 127 (2004).
20. G. J. Kubas, *J. Organomet. Chem.* **635**, 37 (2001).
21. G. S. McGrady, G. Guilera, *Chem. Soc. Rev.* **32**, 383 (2003).
22. R. H. Crabtree, *Acc. Chem. Res.* **23**, 95 (1990).
23. G. J. Kubas, *Science* **314**, 1096 (2006).
24. R. A. Moss, M. S. Platz, M. Jones Jr., Eds., *Reactive Intermediate Chemistry* (Wiley, New York, 2004).
25. D. Bourissou, O. Guerret, F. P. Gabbaï, G. Bertrand, *Chem. Rev.* **100**, 39 (2000).
26. V. Lavallo *et al.*, *J. Am. Chem. Soc.* **126**, 8670 (2004).
27. V. Lavallo, Y. Canac, C. Praesang, B. Donnadieu, G. Bertrand, *Angew. Chem. Int. Ed.* **44**, 5705 (2005).
28. A. J. Arduengo III, R. L. Harlow, M. Kline, *J. Am. Chem. Soc.* **113**, 361 (1991).
29. F. E. Hahn, *Angew. Chem. Int. Ed.* **45**, 1348 (2006).
30. M. K. Denk, J. M. Rodezno, S. Gupta, A. J. Lough, *J. Organomet. Chem.* **617–618**, 242 (2001).
31. D. A. Dixon, A. J. Arduengo III, K. D. Dobbs, D. V. Khasnis, *Tetrahedron Lett.* **36**, 645 (1995).
32. V. Lavallo, Y. Canac, B. Donnadieu, W. W. Schoeller, G. Bertrand, *Angew. Chem. Int. Ed.* **45**, 3488 (2006).
33. M. J. Frisch *et al.*, *Gaussian 03* (Gaussian, Wallingford, CT, revision C.02, 2004).
34. In a first approximation, the singlet-triplet energy gap parallels the HOMO-LUMO (lowest unoccupied molecular orbital) splitting.
35. Carbenes **1** and **2** are highly moisture sensitive, and the low yields observed are due to the presence of water in the H_2 gas, which gives rise to the H_2O-carbene adducts.
36. Preparation methods and spectroscopic data for compounds **5**, **6a**, **6b**, **7**, **8a**, and **8b** are available on *Science* Online.
37. A. J. Arduengo III *et al.*, *J. Am. Chem. Soc.* **116**, 6641 (1994).
38. R. W. Alder, P. R. Allen, M. Murray, A. G. Orpen, *Angew. Chem. Int. Ed. Engl.* **35**, 1121 (1996).
39. W. A. Herrmann, M. Elison, J. Fischer, C. Köcher, G. R. J. Artus, *Chem. Eur. J.* **2**, 772 (1996).
40. We are grateful to NSF (grant CHE 0518675) and RHODIA for financial support of this work, the University of Bielefeld for computer facilities, the Alexander von Humboldt Foundation for a fellowship (G.D.F.), and A. J. Arduengo for helpful discussions. Metrical data for the solid state structures of **6a** and **8b** are available free of charge from the Cambridge Crystallographic Data Centre under reference numbers CCDC-637184 and CCDC-637185, respectively.

Supporting Online Material

www.sciencemag.org/cgi/content/full/316/5823/439/DC1
Materials and Methods
Figs. S1 and S2
Tables S1 to S4
References and Notes

20 February 2007; accepted 13 March 2007
10.1126/science.1141474